

Water-soluble nano-pearl powder promotes MC3T3-E1 cell differentiation by enhancing autophagy via the MEK/ERK signaling pathway

YANAN CHENG, WENBAI ZHANG, HUI FAN and PU XU

Department of Oral Implantation, Affiliated Haikou Hospital, Xiangya Medical School, Central South University, Hainan Provincial Stomatology Center, Haikou, Hainan 570208, P.R. China

Received September 30, 2017; Accepted February 16, 2018

DOI: 10.3892/mmr.2018.9052

Abstract. Nacre (mother of pearl) is a bioactive material capable of facilitating osteoblast proliferation and differentiation; however, further investigation into the mechanism underlying the effects of nacre on the stimulation of bone differentiation is required. The present study aimed to elucidate the effects of water-soluble nano-pearl powder (WSNNP) on osteoblast differentiation and to examine the underlying mechanisms. A MTT assay revealed that WSNNP (10, 25 and 50 $\mu\text{g/ml}$) may stimulate the viability of preosteoblastic MC3T3-E1 cells and 50 $\mu\text{g/ml}$ WSNNP exhibited the maximum stimulatory effect. Furthermore, WSNNP significantly enhanced the protein expression levels of differentiation markers, including collagen I, runt-related transcription factor 2 (RUNX2), secreted phosphoprotein1 (SPP1) and alkaline phosphatase (ALP) in a dose-dependent manner, which indicated that WSNNP may promote osteoblast differentiation. Subsequently, whether autophagy serves a role in WSNNP-mediated differentiation of osteoblasts was investigated via western blotting and immunofluorescence. The results of the present study demonstrated that WSNNP treatment significantly evoked the expression of autophagy markers, including microtubule-associated light chain 3 (LC3)II/I, Beclin1 and autophagy-related 7 (ATG7), whereas the autophagy inhibitor 3-methyladenine significantly inhibited WSNNP-induced osteoblast differentiation. Furthermore, the role of WSNNP on the potential signaling pathways that activate autophagy was investigated. The present study reported that WSNNP

may significantly upregulate the mitogen-activated protein kinase kinase (MEK)/extracellular signal-regulated kinase (ERK) signaling pathway. Treatment with the MEK inhibitor U0126 significantly inhibited the protein expression levels of WSNNP-induced differentiation markers, including collagen I, RUNX2, SPP1 and ALP, and autophagy markers, including LC3II/I, Beclin1 and ATG7. Therefore, the findings of the present study suggested that WSNNP may contribute to osteoblast differentiation by enhancing autophagy via the MEK/ERK signaling pathway, thus suggesting a novel direction for optimizing the biological materials in bone implants.

Introduction

Bone remodeling comprises bone-forming osteoblast and bone-resorbing osteoclast processes (1,2). The normal balance between resorption and formation is essential for fracture healing and skeletal development (3). There are four stages of bone formation: Proliferation, differentiation, maturation and mineralization. These stages guide the osteoblasts to gradually differentiate into osteocytes and facilitate osteogenesis (4); therefore, high bioactivity and biocompatibility, osteoconduction and biodegradability are necessary characteristics in an alternative material that may facilitate bone regeneration (5). In the past three decades, various bone substitutes with high biocompatibility and good osteoconduction have been reported and have been applied to repair bone defects (6-9); however, insufficient bioactivity of these materials has restricted the repair process (8). Therefore, high biocompatibility, biodegradability and osteogenic potential are considered desirable for bone tissue engineering.

Nacre (mother of pearl) is a naturally formed composite material constituting inorganic calcium carbonate plates and a complex organic matrix. A previous study demonstrated that nacre exhibits excellent biocompatibility, biodegradability and osteogenic properties, and may be used as a potential biomaterial in tissue engineering (7). Numerous studies have reported that nacre functions to promote osteoblast proliferation and differentiation (10,11). Lamghari *et al* (12) observed the osteogenic potential of nacre *in vitro* and *in vivo*. Asvanund *et al* (13) reported that pearls may promote the

Correspondence to: Dr Pu Xu, Department of Oral Implantation, Affiliated Haikou Hospital, Xiangya Medical School, Central South University, Hainan Provincial Stomatology Center, 43 Renmin Road, Meilan, Haikou, Hainan 570208, P.R. China
E-mail: xupuhn@163.com

Key words: water-soluble nano-pearl powder, autophagy, osteoblast differentiation, mitogen-activated protein kinase kinase/extracellular signal-regulated kinase signaling pathway, mammalian target of rapamycin

osteogenic differentiation of human bone cells by increasing alkaline phosphatase (ALP) and osteocalcin expression *in vitro*. Furthermore, it is possible that nacre contains signaling molecules capable of stimulating the osteogenic pathway in mammalian cells. The organic matrix of nacre has also been suggested to contain biological molecules capable of activating osteoblast activity (14,15). The water-soluble matrix (WSM) of nacre promotes antioxidative and osteogenic differentiation activities in MC3T3-E1 cells (14); however, the purification and classification of WSM is complex, and one of the main goals in the research of nacre is to determine its mechanism for promoting bone differentiation. Therefore, it is important to investigate the most effective factors of extracted pearl powder and the mechanism by which it effectively improves bone formation.

The present study aimed to investigate the role of water-soluble nano-pearl powder (WSNNP) on osteoblast differentiation and its underlying mechanisms. The results indicated that WSNNP stimulated osteoblast differentiation and enhanced cell mineralization by activating the extracellular signal-regulated kinase (ERK)-autophagy signaling pathway. The present study provides evidence of a promising biological material for bone-grafting procedures.

Materials and methods

Scanning electron microscopy (SEM) and transmission electron microscopy (TEM). The nano-pearl powder (NNP) samples were sent to the Southern Medical University (Shenzhen, China) to verify the presence of NNP by SEM (S-3000; Hitachi, Ltd., Tokyo, Japan) and TEM (JEM-2100; JEOL, Ltd., Tokyo, Japan).

Cell culture. MC3T3-E1 cells can differentiate into osteoblasts and induce mineralization, and were purchased from the American Type Culture Collection (Manassas, VA, USA). The cells were cultured in phenol-red-free α -Minimum Essential medium (Thermo Fisher Scientific, Inc., Waltham, MA, USA) supplemented with 10% fetal bovine serum (Thermo Fisher Scientific, Inc.), 5 mM β -glycerophosphate and 25 mg/ml ascorbic acid at 37°C in an atmosphere containing 5% CO₂.

Cell treatment. NNP (100 mg; Jingrun Pearl Biological, Inc., Hainan, China) was dissolved in 100 ml PBS, magnetically stirred for 24 h at 4°C and centrifuged at 30,000 \times g at 4°C for 20 min. The supernatant was freeze-dried at -80°C to obtain the WSNNP in powdered form. The freeze-dried powder was then dissolved in PBS and a bicinchoninic acid (BCA) protein assay was performed. Subsequently treatment for 48 h with 0, 10, 25 and 50 μ g protein/ml WSNNP was used for further study (14). An autophagy inhibitor 3-methyladenine (3-MA), and a mitogen-activated protein kinase kinase (MEK) signaling inhibitor, U0126, were obtained from Sigma-Aldrich (Merck KGaA, Darmstadt, Germany). WSNNP protein (25 μ g/ml), and either 5 mmol 3-MA or 15 μ M U0126, were added to the cells and incubated for 48 h at 37°C prior to further analysis.

Immunofluorescence assay. For the immunofluorescence assay, 4% formaldehyde was used to fix the cells (1 \times 10⁵ cells/ml)

onto coverslips for 30 min at 4°C, followed by the addition of PBS containing 0.5% Triton-X-100 to the coverslips for 20 min to increase permeability. The cells were then blocked in 5% non-fat milk in Tris-buffered saline with Tween-20 (TBST; 0.05% Tween-20) for 60 min at room temperature and incubated with anti-Beclin1 antibody (ab62472; 1:100; Abcam, Cambridge, UK) at 4°C overnight. The cells were then exposed to Cy3 goat anti-rabbit immunoglobulin G (sc-2004; 1:200; Santa Cruz Biotechnology, Inc., Dallas, TX, USA) at 37°C for 1 h. The coverslips were stained with DAPI (sc-3598; 1:1,000; Santa Cruz Biotechnology, Inc.) for 2 min and mounted on slides using anti-fade mounting medium. Immunofluorescence images were captured using the Nikon ECLIPSE 80i microscope (Nikon Corporation, Tokyo, Japan).

MTT assay. The MTT assay was performed every 24 h to measure cell viability. After the indicated treatment, 3 \times 10³ cells were seeded into each well of 96-well plates. Briefly, 4 μ l MTT (Sigma-Aldrich; Merck KGaA) was added to the cells, which were incubated for 4 h at 37°C. Subsequently, 150 μ l dimethyl sulfoxide (Sigma-Aldrich; Merck KGaA) was used to dissolve the formazan crystals and the absorbance was measured at 570 nm using a microplate reader.

Western blotting. RIPA lysis buffer (P002A, Auragene, Changsha, China) was added to the indicated cells to extract the proteins. The protein concentration was then measured using a BCA Protein Assay kit (Auragene, Changsha, China); 50 μ g protein was separated by 12% SDS-PAGE and blotted onto 0.22- μ m nitrocellulose membranes. The membranes were blocked with 5% milk-TBS for 2 h at room temperature and were incubated with the following primary antibodies overnight at 4°C: Mouse monoclonal anti-collagen I (ab138492; 1:1,000; Abcam), mouse monoclonal anti-secreted phosphoprotein 1 (SPP1; AM4093; 1:1,000; Abzoom Biolabs, Inc., Dallas, TX, USA), rabbit polyclonal anti-runt-related transcription factor 2 (RUNX2; ab3931; 1:500; Abcam), rabbit polyclonal anti-microtubule-associated light chain 3 (LC3)II/I (ab51520; 1:500; Abcam), rabbit polyclonal anti-Beclin1 (ab62472; 1:1,000; Abcam) and rabbit polyclonal anti-autophagy-related 7 (ATG7; 10088-2-AP; 1:1,000; ProteinTech Group, Inc., Chicago, IL, USA), rabbit polyclonal anti-ERK (YM0244; 1:1,000; ImmunoWay Biotechnology Co., Plano, TX, USA), rabbit polyclonal anti-phosphorylated (p)-ERK (YP0497; 1:1,000; ImmunoWay Biotechnology Co.), rabbit polyclonal anti-MEK (YM0435; 1:1,000; ImmunoWay Biotechnology Co.), rabbit polyclonal anti-p-MEK (YP0169; 1:500; ImmunoWay Biotechnology Co.), rabbit polyclonal anti-mammalian target of rapamycin (mTOR; YT2913; 1:1,000; ImmunoWay Biotechnology Co.), rabbit polyclonal anti-p-mTOR (YP0176; 1:200; ImmunoWay Biotechnology Co.), rabbit polyclonal anti-p70 S6 kinase (p70S6K; ab9366; 1:1,000; Abcam), rabbit polyclonal anti-p-p70S6K (ab126818; 1:200; Abcam) and mouse monoclonal anti- β -actin (ab8226; 1:2,000; Abcam). The membranes were then washed with TBST and incubated with the appropriate horseradish peroxidase-conjugated secondary antibodies (goat anti-rabbit; sc-2004; 1:2,000 and goat anti-mouse; sc-2039 1:2,000; Santa Cruz Biotechnology, Inc.) for 1 h at 37°C. Finally, the membranes were exposed to enhanced chemiluminescence

(P020WB; Auragene, Changsha, China) for visualization and the optical density of the objective protein levels was analyzed by densitometry using Image-Pro Plus version 6.0 (Bio-Rad Laboratories, Inc., Hercules, CA, USA).

ALP activity. Triton X-100 (1%) was used to lyse the cells for 30 min at 4°C and centrifuged at 8,000 x g for 5 min at 4°C. The protein was extracted from supernatant and the ALP Assay kit (ab83369; Abcam) was used to detect ALP activity, according to the manufacturer's protocol.

ALP staining. MC3T3-E1 cells (1x10⁵ cells/ml) were treated with 25 µg/ml WSNNP for 3 days at 37°C. The ALP Staining kit (D001-2; Nanjing Jiancheng Bioengineering Institute, Nanjing, China) was then used to detect the extent of ALP staining, according to the manufacturer's protocol and the cells examined under a light microscope (AE41; Motic, Xiamen, China).

Alizarin red S staining. MC3T3-E1 cells (1x10⁵ cells/ml) were treated with WSNNP 25 µg/ml for 14 days at 37°C. Subsequently, the Alizarin Red S staining kit (G1450; Beijing Solarbio Science & Technology Co., Ltd., Beijing, China) was used to detect the intensity of Alizarin Red S staining according to the manufacturer' protocol and the cells examined under a light microscope (AE41; Motic).

Statistical analysis. GraphPad Prism 5 (GraphPad Software, Inc., La Jolla, CA, USA) was used for statistical analyses, and the data are presented as the means ± standard deviation. One-way analysis of variance and the Bonferroni post hoc test were used to analyze data from more than two groups. An unpaired two-tailed Student's t-test was used to analyze data from two groups. P<0.05 was considered to indicate a statistically significant difference.

Results

WSNNP enhances the differentiation and maturation of cultured MC3T3-E1 cells. SEM and TEM were used to confirm the presence of WSNNP prepared from the NNP (Fig. 1A and B). Subsequently, the effects of WSNNP on the viability of MC3T3-E1 cells were determined using the MTT assay. The present study revealed that 10, 25 and 50 µg/ml WSNNP stimulated MC3T3-E1 cell viability, and of these concentrations, 50 µg/ml WSNNP had the maximum effect (Fig. 1C). To investigate the effects of WSNNP on osteoblast differentiation, western blotting and ALP activity assays were performed. The results indicated that increases in the expression levels of collagen I, SPP1 and RUNX2 may have promoted osteogenic differentiation. Collagen I is known to stimulate cell migration, proliferation and osteogenic differentiation of rat bone-marrow stromal cells (15). SPP1, also known as osteopontin, is a marker of the later period of osteoblast mineralization, whereas RUNX2 acts as the key regulator of bone formation by regulating osteoblast differentiation (16). In the present study, WSNNP treatment significantly enhanced the protein expression levels of collagen I, SPP1 and RUNX2 in a dose-dependent manner (Fig. 1D and E). ALP activity served as an initial indicator of osteoblast differentiation; WSNNP

treatment also increased ALP activity and Alizarin Red S staining in a time- and dose-dependent manner (Fig. 1F-H). These results suggested that WSNNP may promote osteoblast proliferation and differentiation.

WSNNP contributes to MC3T3-E1 cell differentiation by enhancing autophagy. To understand the potential mechanism by which WSNNP regulates osteoblast differentiation, and considering the close association between autophagy and bone development, the present study investigated whether WSNNP may regulate autophagy. MC3T3-E1 cells were treated with various concentrations of WSNNP (10, 25 and 50 µg/ml); immunofluorescence and western blotting were conducted to measure the expression levels of autophagy markers. The results of the present study revealed that WSNNP enhanced Beclin1 fluorescence (Fig. 2A). Increasing concentrations of WSNNP also upregulated the expression levels of LC3II/I, Beclin1 and ATG7, which are key molecules of autophagy signaling, with the exception of 50 µg/ml WSNNP on the expression of LC3II/I (Fig. 2B and C). These findings indicated that WSNNP may stimulate autophagy.

The present study also investigated whether autophagy was required for WSNNP-mediated osteoblast differentiation using 25 µg/ml WSNNP. Briefly, 3-MA was used as an autophagy inhibitor; autophagy and osteoblast differentiation of MC3T3-E1 cells were evaluated using western blotting, immunofluorescence and ALP activity assays in the presence of WSNNP treatment with or without 3-MA. Western blotting results demonstrated that the expression levels of LC3II/I, Beclin1 and ATG7 were significantly inhibited by 3-MA compared with in cells treated with WSNNP alone (Fig. 2D and E). Immunofluorescence assays revealed that the expression levels of Beclin1 were enhanced in the WSNNP-treated group and reduced in the 3-MA and WSNNP cotreatment group (Fig. 2F). The results of the present study indicated that 3-MA significantly inhibited WSNNP-induced autophagy. Notably, cotreatment with WSNNP and 3-MA also significantly downregulated the protein expression levels of collagen I, SPP1 and RUNX2 compared with in cells treated with WSNNP alone (Fig. 3A and B). ALP activity was also significantly inhibited by 3-MA compared with in the WSNNP group, but was enhanced by WSNNP alone (Fig. 3C). These results suggested that WSNNP may contribute to MC3T3-E1 cell differentiation by enhancing autophagy.

WSNNP stimulates MC3T3-E1 cell autophagy via the MEK/ERK signaling pathway. The present study also investigated whether WSNNP may stimulate autophagy via the MEK/ERK signaling pathway. ERK/MEK is a known activator of autophagy (17,18). The present study demonstrated that WSNNP significantly upregulated the phosphorylation levels of ERK and MEK, and inhibited the phosphorylation of mTOR and p70S6K compared with in the control group (Fig. 4A and B). These results suggested that WSNNP may stimulate autophagy via the MEK/ERK signaling pathway. To confirm this, the MEK signaling inhibitor, U0126, was employed to inhibit ERK signaling. Autophagy levels were evaluated using western blotting and immunofluorescence, and the potential of osteoblast differentiation was analyzed via western blotting and ALP activity assays. The results of

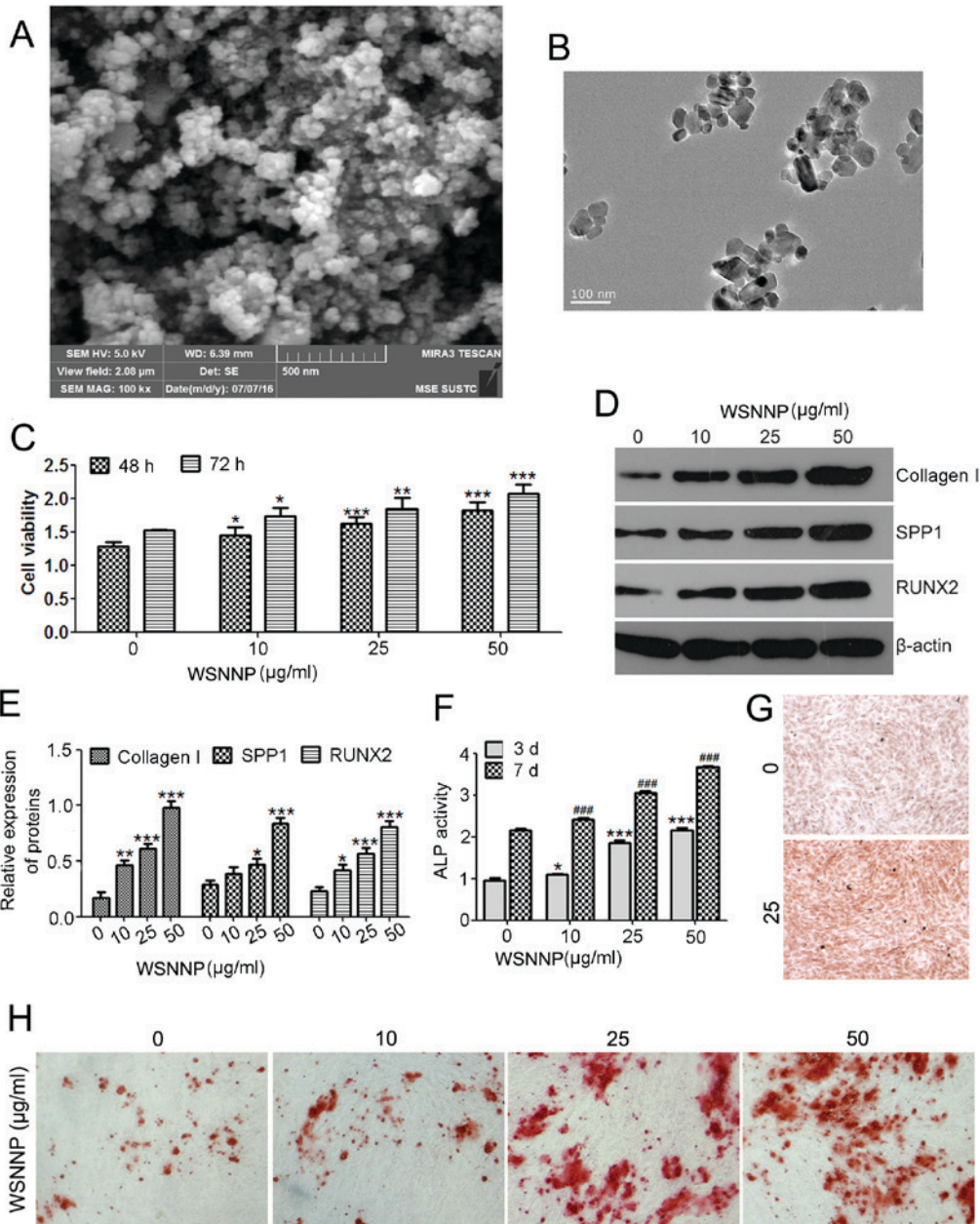


Figure 1. WSNNP stimulates MC3T3-E1 cell viability and differentiation. NNP observed by (A) scanning electron microscopy and (B) transmission electron microscopy. (C) MTT assay was performed to measure cell viability following WSNNP treatment (0, 10, 25 and 50 µg/ml) for 48 and 72 h. (D and E) Expression levels of collagen I, SPP1 and RUNX2 were determined by western blotting following WSNNP treatment (0, 10, 25 and 50 µg/ml) for 48 h. (F) ELISA assay was used to detect the ALP expression following treatment with WSNNP (0, 10, 25 and 50 µg/ml) for 3 and 7 days. (G) ALP staining of cells following WSNNP treatment (0 and 25 µg/ml) for 3 days (magnification, x200). (H) Alizarin red S staining of cells treated with WSNNP (0, 10, 25 and 50 µg/ml) for 14 days (magnification, x200). Data are presented as the means ± standard deviation, n=3. *P<0.001, **P<0.01, ***P<0.05 and ****P<0.001 vs. non-WSNNP-treated cells on day 7. ALP, alkaline phosphatase; RUNX2, runt-related transcription factor 2; SPP1, secreted phosphoprotein1; WSNNP, water-soluble nano-pearl powder.

the present study revealed that U0126 significantly diminished WSNNP-mediated autophagy, which was determined by the decrease in LC3II/I, Beclin1 and ATG7 expression levels (Fig. 4C and D). In addition, inhibition of ERK signaling by U0126 significantly attenuated the expression of collagen I, SPP1 and RUNX2, and ALP activity, which were upregulated by WSNNP (Fig. 4E and F). These results revealed that WSNNP may promote MC3T3-E1 cell differentiation by enhancing autophagy via the MEK/ERK/mTOR signaling pathway.

Discussion

In the present study, WSNNP promoted osteoblast differentiation in a time- and dose-dependent manner. Further investigation revealed that WSNNP contributed to osteoblast differentiation by enhancing autophagy via the MEK/ERK signaling pathway. To the best of our knowledge, the present study is the first to report that overactivated autophagy may be a potential mechanism underlying the effects of WSNNP on osteoblast differentiation.

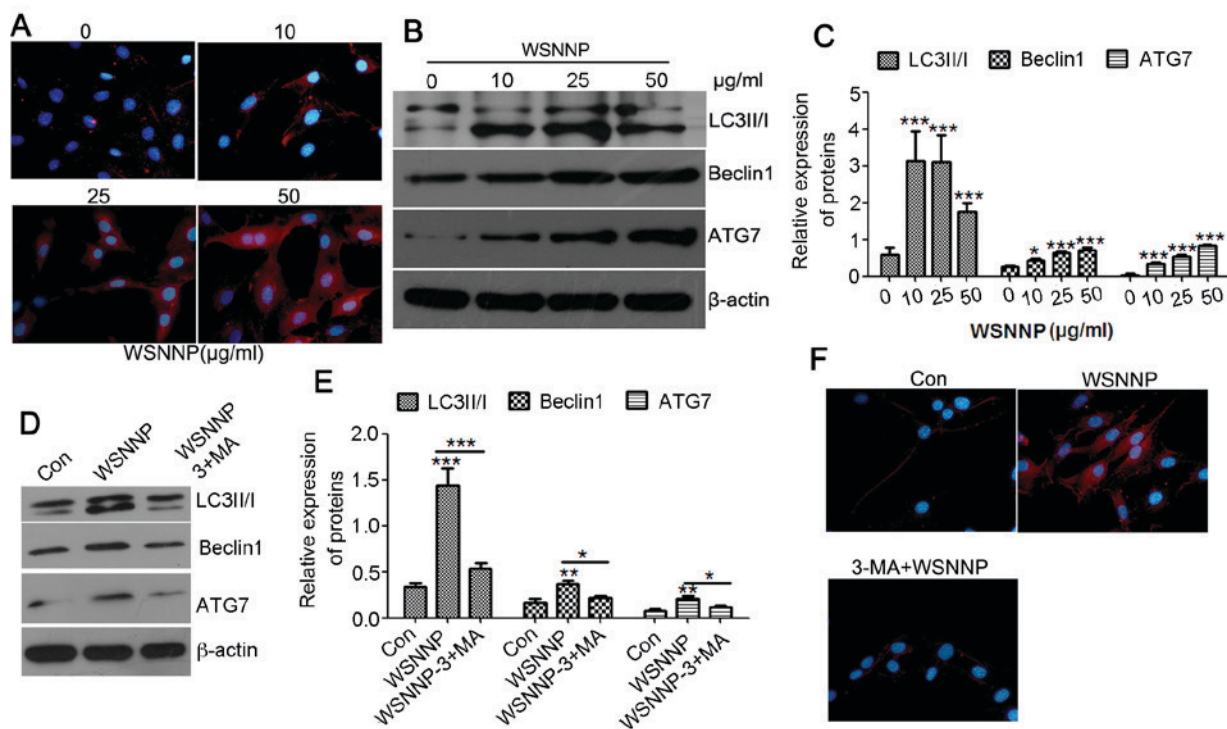


Figure 2. WSNNP stimulates autophagy in MC3T3-E1 cells, which is reversed by 3-MA. (A) Expression of Beclin1 (red) following WSNNP treatment (0, 10, 25 and 50 $\mu\text{g/ml}$) for 48 h in MC3T3-E1 cells was analyzed by an immunofluorescence assay. Blue staining indicates nuclei. Magnification, $\times 400$. (B and C) Protein expression levels of LC3II/I, Beclin1 and ATG7 were detected by western blotting following WSNNP treatment (0, 10, 25 and 50 $\mu\text{g/ml}$) for 48 h. (D and E) LC3II/I, Beclin1 and ATG7 expression levels were detected by western blotting following treatment with 25 $\mu\text{g/ml}$ WSNNP, with or without 5 mmol 3-MA, for 48 h. (F) Immunofluorescence was performed to measure the expression of Beclin1 (red) following treatment with 25 $\mu\text{g/ml}$ WSNNP, with or without 5 mmol 3-MA, for 48 h in MC3T3-E1 cells. Blue staining indicates nuclei. Magnification, $\times 400$. Data are presented as the means \pm standard deviation, $n=3$. $^{***}P<0.001$, $^{**}P<0.01$ and $^{*}P<0.05$ vs. non-WSNNP-treated cells at 48 h. 3-MA, 3-methyladenine; ATG7, autophagy-related 7; Con, control; LC3, microtubule-associated light chain 3; WSNNP, water-soluble nano-pearl powder.

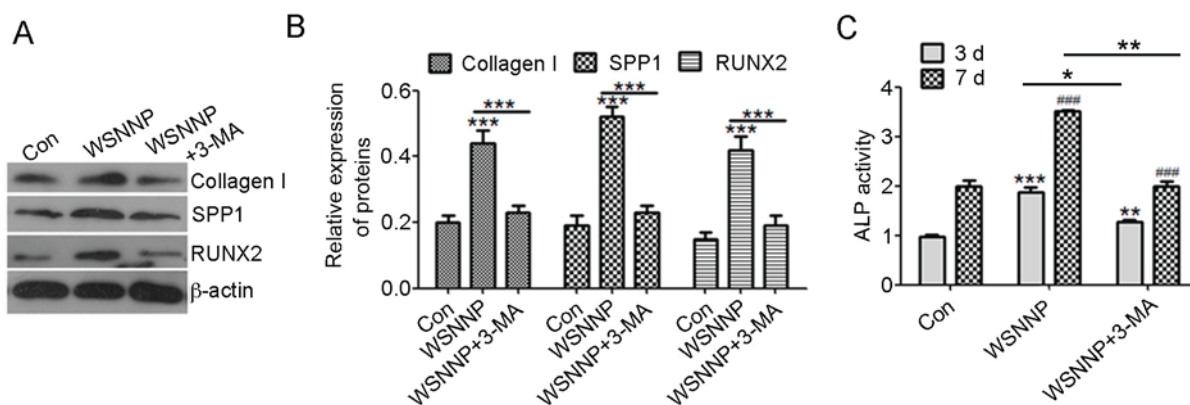


Figure 3. 3-MA reverses WSNNP-mediated differentiation of MC3T3-E1 cells. (A and B) Collagen I, SPP1 and RUNX2 expression levels were measured by western blotting following treatment with 25 $\mu\text{g/ml}$ WSNNP, in the presence or absence of 5 mmol 3-MA, for 48 h. (C) ELISA was used to detect ALP activity following treatment with 25 $\mu\text{g/ml}$ WSNNP, with or without 5 mmol 3-MA, for 3 and 7 days. Data are presented as the means \pm standard deviation, $n=3$. $^{***}P<0.001$, $^{**}P<0.01$ and $^{*}P<0.05$. $^{###}P<0.001$ vs. non-WSNNP-treated cells on day 7. 3-MA, 3-methyladenine; ALP, alkaline phosphatase; Con, control; RUNX2, runt-related transcription factor 2; SPP1, secreted phosphoprotein1; WSNNP, water-soluble nano-pearl powder.

Nacre has been demonstrated to promote osteoblast differentiation and bone formation *in vitro* and *in vivo* (19,20). Lamghari *et al* (12) demonstrated that 12 weeks following the use of nacre powder for treating loss of vertebral bone in sheep, newly matured bone trabeculae occupied the experimental cavity, which indicated bone formation. The water-soluble extract of nacre also resulted in ALP enhancement in bone marrow cells (21). A series of studies revealed

that peptides (14-57 Da) of nacre may serve a role in oxidative activity and as proteinase inhibitors (22-25). However, Duplat *et al* (26) suggested that the small molecules of water soluble nacre may decrease bone resorption by inhibiting osteoclast cathepsin K. Conversely, nacre molecules exposed to MC3T3-E1 cells were revealed to significantly upregulate the mRNA expression levels of collagenI, RUNX2 and osteopontin (27), indicating the potential use for *in vivo* bone repair.

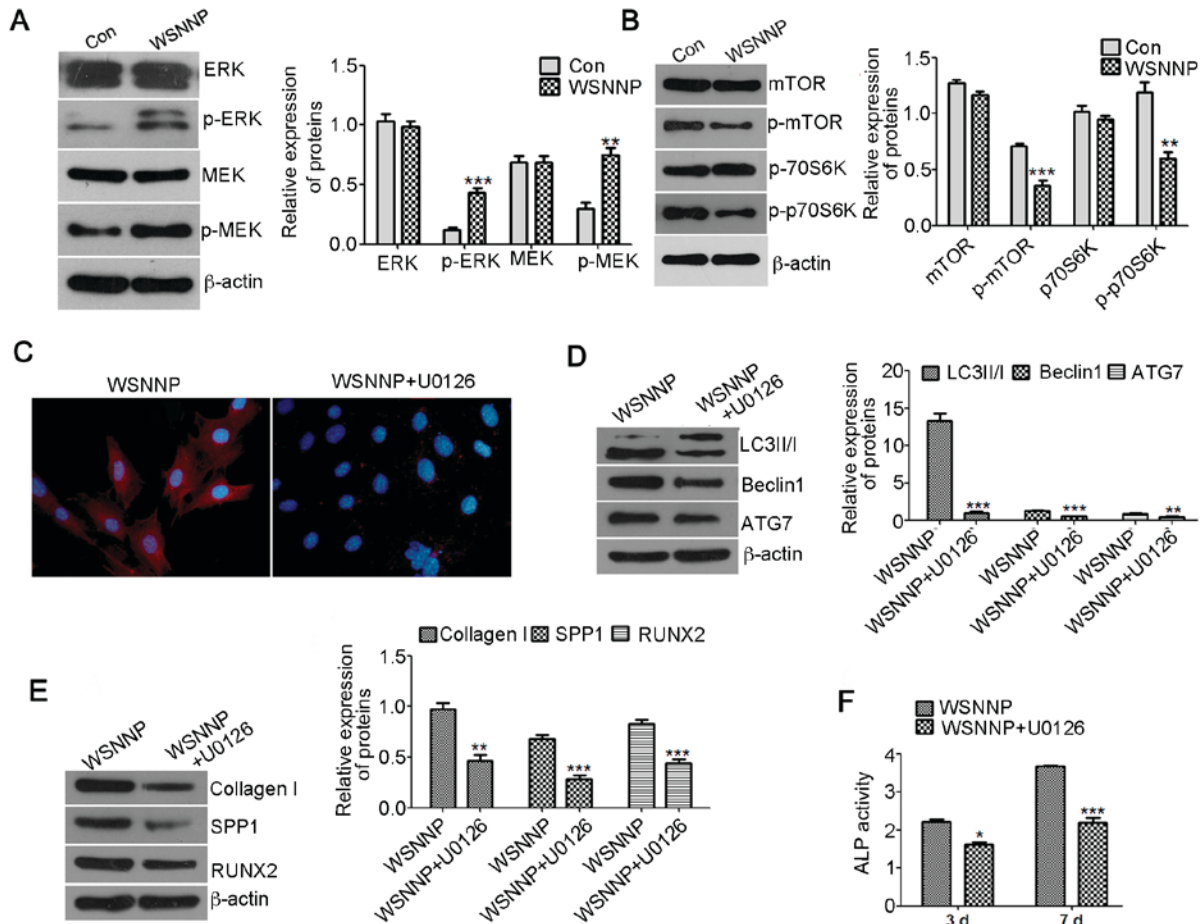


Figure 4. U0126 reverses WSNNP-mediated autophagy and differentiation. (A) Expression levels of ERK, p-ERK, MEK and p-MEK were detected by western blotting following treatment with 25 $\mu\text{g/ml}$ WSNNP for 48 h. β -actin was used as a loading control. (B) mTOR, p-mTOR, p70S6K and p-p70S6K levels were measured by western blotting following treatment with 25 $\mu\text{g/ml}$ WSNNP for 48 h. β -actin was used as a loading control. (C) Expression levels of Beclin1 (red) were assessed by immunofluorescence following treatment of MC3T3-E1 cells with 25 $\mu\text{g/ml}$ WSNNP, in the presence or absence of 15 μM U0126, for 48 h. Blue staining indicates nuclei. Magnification, $\times 400$. (D) LC3II/I, Beclin1 and ATG7 expression levels were assessed by western blotting following treatment with 25 $\mu\text{g/ml}$ WSNNP, in the presence or absence of 15 μM U0126, for 48 h. (E) Expression levels of Collagen I, SPP1 and RUNX2 were detected by western blotting following treatment with 25 $\mu\text{g/ml}$ WSNNP, in the presence or absence of 15 μM , U0126 for 48 h. (F) ALP activity was assessed by ELISA assay following treatment with 25 $\mu\text{g/ml}$ WSNNP, in the presence or absence of 15 μM U0126, for 3 and 7 days. Data are presented as the means \pm standard deviation, $n=3$. *** $P<0.001$, ** $P<0.01$, and * $P<0.05$ vs. non-U0126-treated group. ALP, alkaline phosphatase; Con, control; ERK, extracellular signal-regulated kinase; LC3, microtubule-associated light chain 3; MEK, mitogen-activated protein kinase kinase; mTOR, mammalian target of rapamycin; p, phosphorylated; p70S6K, p70 S6 kinase; RUNX2, runt-related transcription factor 2; SPP1, secreted phosphoprotein1; WSNNP, water-soluble nano-pearl powder.

Laothumthut *et al* (28) demonstrated that WSM promotes the proliferation of human dental pulp cells. The results of these studies are consistent with those of the present study, in which the effects of WSNNP on the differentiation of MC3T3-E1 cells were investigated. More protein may be extracted from WSNNP than micro-pearl powder and significantly increase cell differentiation compared with the water solution of micro-pearl powder (15,607 vs. 985 $\mu\text{g/ml}$, respectively) (data not shown). Additionally, the present study demonstrated that WSNNP may stimulate MC3T3-E1 cell differentiation and enhance the protein expression levels of collagen I, SPP1 and RUNX2, and ALP activity; however, the mechanism by which WSNNP stimulates MC3T3-E1 cell differentiation requires further investigation.

Autophagy is a mechanism by which cells are protected and regulated to allow the removal of excess organelles, in order to maintain stability of the cell environment. Numerous factors, including inflammation, immune response, medication and external stimuli, may lead to cell autophagy (29-31).

It has previously been reported that autophagy may serve a latent role in the pathogenesis of osteogenesis (32), and activation of autophagy may inhibit cadmium-induced osteoblast apoptosis (33). Nollet *et al* (34) revealed that autophagy is activated during bone mineralization and that the inhibition of autophagy by interfering with relative gene expression associated with autophagy in mice may reduce bone mineralization. In addition, autophagy serves an important role in osteoblast differentiation. Insulin-like growth factor-1 and insulin-like growth factor-binding protein 2 stimulate 5'adenosine monophosphate-activated protein kinase and activate autophagy, which are important factors for osteoblast differentiation (35). Notably, fibroblast growth factor (FGF)18, via FGF receptor 4 and c-Jun N-terminal kinase-dependent activation of autophagy, promotes bone growth (36). The results of the present study demonstrated that WSNNP treatment enhanced autophagy. However, co-treatment of MC3T3-E1 cells with WSNNP and 3-MA downregulated the protein expression levels of collagen I, SPP1 and RUNX2, and ALP activity,

compared with WSNNP treatment alone. The present study revealed that WSNNP stimulated osteoblast differentiation by enhancing autophagy and that autophagy may serve an important role in MC3T3-E1 cell differentiation.

The ERK/MEK signaling pathway is known to be involved in autophagy; one study reported the presence of the autophagy marker Beclin1 and the conversion of LC3-I to LC3-II, activated by ERK-dependent autophagic activity (37). Liu *et al* (38) also demonstrated that autophagy may be evoked by lithium chloride to promote spinal cord injury through the ERK-dependent pathway. Wang *et al* (39) demonstrated that the MEK inhibitor U0126 attenuates ischemia/reperfusion-induced apoptosis and autophagy in the myocardium via the ERK/MEK/early growth response protein 1 pathway. The present study demonstrated that WSNNP may activate the phosphorylation of ERK and MEK, and that U0126 may reverse WSNNP-induced MC3T3-E1 cell autophagy and differentiation. Therefore, WSNNP may promote osteoblast differentiation by activating ERK-associated autophagy. However, only the WSNNP-affected signaling pathway associated with osteoblast differentiation was investigated in the present study. There may be crosstalk between WSNNP and MEK; however, further investigation is required.

In conclusion, in the present study, a novel mechanism by which WSNNP promotes osteoblast differentiation by regulating autophagy via the MEK/ERK signaling pathway was demonstrated. These findings may provide insight for optimization of biological materials employed for bone implants.

Acknowledgements

Not applicable.

Funding

The present study was supported by the Key Research and Development Projects of Hainan Province (grant no. ZDYF2016018) and Natural Science Foundation of Hainan Province (grant nos. 814378 and 20168313).

Availability of data and materials

All data generated or analyzed during this study are included in this published article.

Authors' contributions

Study design by YC and PX, statistical analysis by WZ, data interpretation by HF and manuscript writing and revision by PX.

Ethics approval and consent to participate

Not applicable.

Consent for publication

Not applicable.

Competing interests

The authors declare that they have no competing interests.

References

1. Maruotti N, Corrado A and Cantatore FP: Osteoblast role in osteoarthritis pathogenesis. *J Cell Physiol* 232: 2957-2963, 2017.
2. Saint-Pastou Terrier C and Gasque P: Bone responses in health and infectious diseases: A focus on osteoblasts. *J Infect* 75: 281-292, 2017.
3. Dallas SL, Prideaux M and Bonewald LF: The osteocyte: An endocrine cell ... and more. *Endocr Rev* 34: 658-690, 2013.
4. Insua A, Monje A, Wang HL and Miron RJ: Basis of bone metabolism around dental implants during osseointegration and peri-implant bone loss. *J Biomed Mater Res A* 105: 2075-2089, 2017.
5. Jazayeri HE, Tahriri M, Razavi M, Khoshroo K, Fahimipour F, Dashtimoghadam E, Almeida L and Tayebi L: A current overview of materials and strategies for potential use in maxillofacial tissue regeneration. *Mater Sci Eng C Mater Biol Appl* 70: 913-929, 2017.
6. Uzeda MJ, de Brito Resende RF, Sartoretto SC, Alves ATNN, Granjeiro JM and Calasans-Maia MD: Randomized clinical trial for the biological evaluation of two nanostructured biphasic calcium phosphate biomaterials as a bone substitute. *Clin Implant Dent Relat Res* 19: 802-811, 2017.
7. Flausse A, Henrionnet C, Dossot M, Dumas D, Hupont S, Pinzano A, Mainard D, Galois L, Magdalou J, Lopez E, *et al*: Osteogenic differentiation of human bone marrow mesenchymal stem cells in hydrogel containing nacre powder. *J Biomed Mater Res A* 101: 3211-3218, 2013.
8. Pilliar RM, Filiaggi MJ, Wells JD, Grynblas MD and Kandel RA: Porous calcium polyphosphate scaffolds for bone substitute applications-in vitro characterization. *Biomaterials* 22: 963-972, 2001.
9. Lopez E, Le Faou A, Borzeix S and Berland S: Stimulation of rat cutaneous fibroblasts and their synthetic activity by implants of powdered nacre (mother of pearl). *Tissue Cell* 32: 95-101, 2000.
10. Shen Y, Zhu J, Zhang H and Zhao F: In vitro osteogenic activity of pearl. *Biomaterials* 27: 281-287, 2006.
11. Mouries LP, Almeida MJ, Milet C, Berland S and Lopez E: Bioactivity of nacre water-soluble organic matrix from the bivalve mollusk *Pinctada maxima* in three mammalian cell types: Fibroblasts, bone marrow stromal cells and osteoblasts. *Comp Biochem Physiol B Biochem Mol Biol* 132: 217-229, 2002.
12. Lamghari M, Almeida MJ, Berland S, Huet H, Laurent A, Milet C and Lopez E: Stimulation of bone marrow cells and bone formation by nacre: In vivo and in vitro studies. *Bone* 25 (2 Suppl): 91S-94S, 1999.
13. Asvanund P, Chunhabundit P and Suddhasthira T: Potential induction of bone regeneration by nacre: An in vitro study. *Implant Dent* 20: 32-39, 2011.
14. Chaturvedi R, Singha PK and Dey S: Water soluble bioactives of nacre mediate antioxidant activity and osteoblast differentiation. *PLoS One* 8: e84584, 2013.
15. Hesse E, Hefferan TE, Tarara JE, Haasper C, Meller R, Krettek C, Lu L and Yaszemski MJ: Collagen type I hydrogel allows migration, proliferation, and osteogenic differentiation of rat bone marrow stromal cells. *J Biomed Mater Res A* 94: 442-449, 2010.
16. Leboy PS: Regulating bone growth and development with bone morphogenetic proteins. *Ann N Y Acad Sci* 1068: 14-18, 2006.
17. Wang J, Whiteman MW, Lian H, Wang G, Singh A, Huang D and Denmark T: A non-canonical MEK/ERK signaling pathway regulates autophagy via regulating Beclin 1. *J Biol Chem* 284: 21412-21424, 2009.
18. Cagnol S and Chambard JC: ERK and cell death: Mechanisms of ERK-induced cell death-apoptosis, autophagy and senescence. *FEBS J* 277: 2-21, 2010.
19. Wang X, Liu S, Xie L, Zhang R and Wang Z: *Pinctada fucata* mantle gene 3 (PFMG3) promotes differentiation in mouse osteoblasts (MC3T3-E1). *Comp Biochem Physiol B Biochem Mol Biol* 158: 173-180, 2011.
20. Liu Y, Huang Q and Feng Q: 3D scaffold of PLLA/pearl and PLLA/nacre powder for bone regeneration. *Biomed Mater* 8: 65001, 2013.
21. Almeida MJ, Milet C, Peduzzi J, Pereira L, Haigle J, Barthelemy M and Lopez E: Effect of water-soluble matrix fraction extracted from the nacre of *Pinctada maxima* on the alkaline phosphatase activity of cultured fibroblasts. *J Exp Zool* 288: 327-334, 2000.
22. Bedouet L, Marie A, Dubost L, Péduzzi J, Duplat D, Berland S, Puisségur M, Boulzague H, Rousseau M, Milet C and Lopez E: Proteomics analysis of the nacre soluble and insoluble proteins from the oyster *Pinctada margaritifera*. *Mar Biotechnol (NY)* 9: 638-649, 2007.

23. Bédouet L, Rusconi F, Rousseau M, Duplat D, Marie A, Dubost L, Le Ny K, Berland S, Péduzzi J and Lopez E: Identification of low molecular weight molecules as new components of the nacre organic matrix. *Comp Biochem Physiol B Biochem Mol Biol* 144: 532-543, 2006.
24. Bedouet L, Duplat D, Marie A, Dubost L, Berland S, Rousseau M, Milet C and Lopez E: Heterogeneity of proteinase inhibitors in the water-soluble organic matrix from the oyster nacre. *Mar Biotechnol (NY)* 9: 437-449, 2007.
25. Oliveira DV, Silva TS, Cordeiro OD, Cavaco SI and Simes DC: Identification of proteins with potential osteogenic activity present in the water-soluble matrix proteins from *Crassostrea gigas* nacre using a proteomic approach. *ScientificWorldJournal* 2012: 765909, 2012.
26. Duplat D, Gallet M, Berland S, Marie A, Dubost L, Rousseau M, Kamel S, Milet C, Brazier M, Lopez E and Bédouet L: The effect of molecules in mother-of-pearl on the decrease in bone resorption through the inhibition of osteoclast cathepsin K. *Biomaterials* 28: 4769-4778, 2007.
27. Rousseau M, Boulzaguet H, Biagianni J, Duplat D, Milet C, Lopez E and Bédouet L: Low molecular weight molecules of oyster nacre induce mineralization of the MC3T3-E1 cells. *J Biomed Mater Res A* 85: 487-497, 2008.
28. Laothumthut T, Jantararat J, Paemane A, Roytrakul S and Chunhabundit P: Shotgun proteomics analysis of proliferating STRO-1-positive human dental pulp cell after exposure to nacreous water-soluble matrix. *Clin Oral Investig* 19: 261-270, 2015.
29. De Nunzio C, Giglio S, Stoppacciaro A, Gacci M, Cirombella R, Luciani E, Tubaro A and Vecchione A: Autophagy deactivation is associated with severe prostatic inflammation in patients with lower urinary tract symptoms and benign prostatic hyperplasia. *Oncotarget* 8: 50904-50910, 2017.
30. Takashi O and Matsu A: Autophagy. *Arerugi* 66: 1018-1019, 2017 (In Japanese).
31. Shetty R, Sharma A, Pahuja N, Chevoor P, Padmajan N, Dhamodaran K, Jayadev C, M M A Nuijts R, Ghosh A and Nallathambi J: Oxidative stress induces dysregulated autophagy in corneal epithelium of keratoconus patients. *PLoS One* 12: e184628, 2017.
32. Piemontese M, Onal M, Xiong J, Han L, Thostenson JD, Almeida M and O'Brien CA: Low bone mass and changes in the osteocyte network in mice lacking autophagy in the osteoblast lineage. *Sci Rep* 6: 24262, 2016.
33. Liu W, Dai N, Wang Y, Xu C, Zhao H, Xia P, Gu J, Liu X, Bian J, Yuan Y, *et al*: Role of autophagy in cadmium-induced apoptosis of primary rat osteoblasts. *Sci Rep* 6: 20404, 2016.
34. Nollet M, Santucci-Darmanin S, Breuil V, Al-Sahlanee R, Cros C, Topi M, Momier D, Samson M, Pagnotta S, Cailleteau L, *et al*: Autophagy in osteoblasts is involved in mineralization and bone homeostasis. *Autophagy* 10: 1965-1977, 2014.
35. Xi G, Rosen CJ and Clemmons DR: IGF-I and IGFBP-2 stimulate AMPK activation and autophagy, which are required for osteoblast differentiation. *Endocrinology* 157: 268-281, 2016.
36. Cinque L, Forrester A, Bartolomeo R, Svelto M, Venditti R, Montefusco S, Polishchuk E, Nusco E, Rossi A, Medina DL, *et al*: FGF signalling regulates bone growth through autophagy. *Nature* 528: 272-275, 2015.
37. Cheng Y, Qiu F, Tashiro S, Onodera S and Ikejima T: ERK and JNK mediate TNF α -induced p53 activation in apoptotic and autophagic L929 cell death. *Biochem Biophys Res Commun* 376: 483-488, 2008.
38. Liu P, Zhang Z, Wang Q, Guo R and Mei W: Lithium chloride facilitates autophagy following spinal cord injury via ERK-dependent pathway. *Neurotox Res* 32: 535-543, 2017.
39. Wang A, Zhang H, Liang Z, Xu K, Qiu W, Tian Y, Guo H, Jia J, Xing E, Chen R, *et al*: U0126 attenuates ischemia/reperfusion-induced apoptosis and autophagy in myocardium through MEK/ERK/EGR-1 pathway. *Eur J Pharmacol* 788: 280-285, 2016.